LEVEL II

Report ONR-CR

AD A110286

OPTIMAL TERRAIN-FOLLOWING FEEDBACK CONTROL FOR ADVANCED CRUISE MISSILES

Richard F. Whitbeck
Systems Technology, Inc.
Hawthorne, California

Julian Wolkovitch
Aeronautical Consultant Associates
Rancho Palos Verdes, California

Contract N00014-79-C-0657

January 1982

Final Report

Approved for public release; distribution unlimited

Prepared for

Office of Naval Research, 800 N. Quincy St., Arlington, VA 22217

FOREWORD

The research described in this report was supported by The Office of Naval Research under contract number N00014-79-C-0657 with Dr. Robert E. Whitehead as Project Monitor.

TABLE OF CONTENTS

TABLE OF CONTENTS (Continued)

LIST OF FIGURES

LIST OF FIGURES (Continued)

LIST OF TABLES

SECTION I

INTRODUCTION

A. INTRODUCTION

A cruise missile is a vehicle that spends the major portion of its flight at essentially constant altitude and speed. Some cruise missiles are flown at very low altitudes in order to avoid detection. The terrain-following capabilities of such a missile and its guidance system are of importance. It is desirable that the missile should follow closely the contour of the terrain, which may be fixed (land) or time-varying (ocean waves). A previous study (Ref. 1) demonstrated that optimal control theory could usefully be applied to calculate the best achievable accuracy of terrain-following. Reference 1 showed that, even with an optimal guidance system, terrain-following accuracy was limited by considerations of the cruise missile's inertias, airspeed, and aerodynamic configuration. In Ref. 1, attention was focussed on these vehicle-centered considerations, and little effort was devoted to the questions of (i) how such an optimal guidance system can be designed, and (ii) how much improvement in terrain-following accuracy can it achieve over a conventional guidance system. The present report addresses these questions.

B. CONTENTS OF THIS REPORT

Section II summarizes the results presented in Ref. 1. That reference considered three alternative aerodynamic configurations for advanced cruise missiles:

1) Conventional wing plus aft tail; for three alternative wing areas

2) Joined wing (a new type of wing described in Section II); for three alternative wing areas

3) Hybrid, i.e., joined wing plus canard; for one wing area

Section II also discusses the spectra for waves and atmospheric turbulence employed in Ref. 1 and in the present study. Finally, Section II summarizes the principal results obtained in Ref. 1 with regard to the maximum achievable accuracy of terrain-following.

Section III presents the compensation network rquired by the optimal system, and shows that it is stable.

Section IV considers the effects of alternative terrain spectra, comparing the performance of systems optimized for "rolling" and "rough" land terrain versus systems designed to follow waves.

Section V compares the performance of optimal systems versus some systems designed by standard methods (i.e., not employing optimal control theory). It is shown that the latter are much inferior in performance to optimal systems.

Section VI discusses multi-controller systems, e.g. systems employing two or more control surfaces, e.g., elevators and flaps. It is shown that the airframe characteristics limit the performance improvements that can be achieved by multicontroller systems.

Section VII presents the conclusions of the study.

SECTION II

BACKGROUND

A. OBJECTIVES

The work reported herein was performed in conjunction with a companion study dealing with an application of a new type of wing, known as the joined wing (Ref. 1). The joined wing, as a general concept, involves the combination of two wings, a fuselage, and a fin, such that the wings form a diamond shape both in plan view and front view (see, for example, Fig. 1 overleaf).

The specific application of Ref. 1 treats an advanced cruise missile capable of being launche from a standard 21 inch diameter submarine torpedo tube. The specific design goals were:

- Low wave (or terrain) clearance to avoid detection.
- Low radar signature to avoid detection.
- Robustness of the folded vehicle.
- Reliable, rapid, and symmetric unfolding.
- Simplicity.
- Low cost.
- High sustained "g" capability for terminal maneuvers.
- Long range.
- Cruise at M = 0.7, little emphasis on transonic and supersonic capability.

This report deals with the first of these items; it treats the control laws needed to insure a low wave clearance capability.

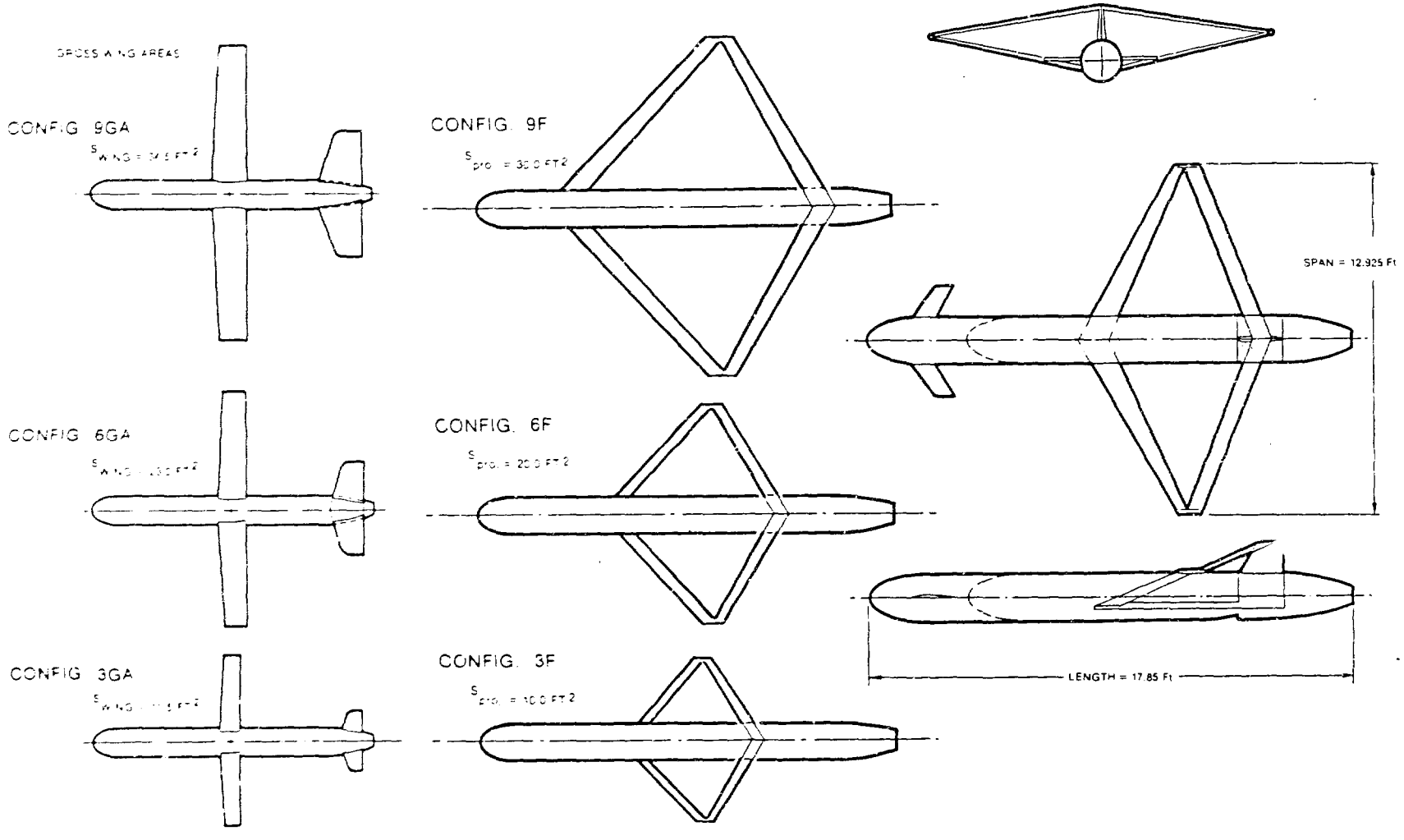

a) Conventional (Aft Tail) b) Joined Wing Configuration c) Hybrid Configuration

Figure 1. Comparison of Conventional and Joined Wing Configurations

B. BACKGROUND

1. The Vehicles

A "cruise missile" is defined as a vehicle that spends the major portion of its flight in a "cruise" mode, i.e., flying at nearly constant altitude and nearly constant speed, using aerodynamic lift to support its weight. The advanced cruise missile configurations discussed in Ref. 1 have launch weights, payloads, and folded dimensions similar to those of Tomahawk class vehicles. The specified low-altitude cruise flight condition (M = 0.7 at sea level) is also similar to that of the Tomahawk. That study was not restricted to vehicles comparable to the Tomahawk; for example, configurations were considered having Tomahawk-like fuselages but wings that are two or three times larger in area than those of the current Tomahawk, to improve maneuverability.

In order to compare the joined wing versus the conventional wing-plus-tail arrangement, 3 configurations of each type were selected. The conventional configurations (denoted 3GA, 6GA, 9GA) had gross wing areas of respectively 11.5, 23.0, and 34.5 ft^2, as shown in Fig. 1a. The joined wing configurations (denoted 3F, 6F, 9F) had gross horizontal projected areas of 10.0, 20.0, and 30.0 ft^2. Figure 1b shows the planforms of these configurations. Configuration 3GA is a baseline configuration, resembling both, but not identical to either the Vought or General Dynamics Tomahawk missiles. Configurations 3GA, 6GA, 9GA have aspect ratios of 9.6: Configurations 3F, 6F, 9F have aspect ratios of 8.35.

An additional configuration was also studied. This configuration, denoted as 6H, is shown in Fig. 1c. It is a hybrid configuration combining a joined wing with a canard.

The configuration numbers denote very approximately the nonsustained maneuver capability of each configuration at M = 0.7, S.L., maximum weight conditions. Thus, Configurations 3GA, 3F can pull approximately 3 g's, Configurations 6F, 6GA, 6H can pull approximately 6 g's, etc. These values are not necessarily sustained g's. The engine thrust may not be sufficient to overcome the airframe drag during a steady maneuver at the designated number of g's.

The initial cruise weight of all configurations is 2864 lb. Thus the more maneuverable configurations sacrifice some fuel because of the larger weight of their lifting surfaces.

2. Airframe Design for Terrain Following

Current and projected cruise missiles employ downward-looking terrain-following systems which measure the missile's clearance above the terrain, i.e., h_c in Fig. 2. A bias setting is incorporated in the guidance logic, corresponding to a desired constant clearance h_B. The difference between h_B and h_c, at any instant, is the height error, h_e. If h_e has a symmetrical statistical distribution, the mean value of h_e, $E(h_e)$, may be assumed to be zero. To achieve stealth h_B should be low, and upward deviations from h_B should be small. With a low h_B, downward deviations from h_B must also be small to reduce the probability of hitting the terrain (usually called "probability of clobber," p_c). Therefore a reasonable criterion for the guidance system is that it should minimize the mean square height error, $E(h_e^2)$. This criterion has the advantage of being mathematically convenient, and it is widely employed in Optimal Control Theory. The theory shows how to compute the guidance system that (for a given airframe) yields minimum $E(h_e^2)$.

While there are advantages to employing minimum $E(h_e^2)$ as a criterion for terrain following, it should be realized that the minimum $E(h_e^2)$ system is only an approximation to the minimum p_c system. This is because

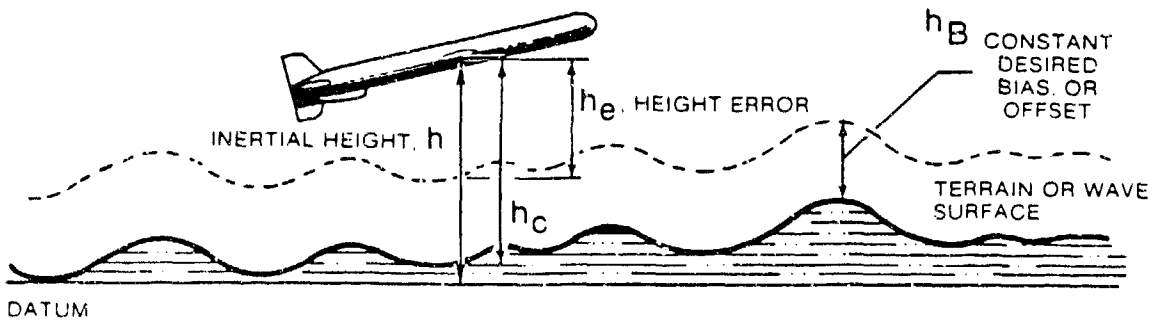

Figure 2. Cruise Missile Flying Above Terrain

p_c depends on the frequency characteristics of h_e as well as its statistical amplitude distribution. For example, consider two Gaussian h_e time histories, having identical $E(h_e^2)$ but with the first having a higher bandwidth than the second. For equal flight durations, the high-bandwidth h_e will have the greater number of exceedances of any specified boundary value. Although $E(h_e^2)$ is a less precise measure of system merit than p_c, it provides a valid and cost-effective basis for comparison of alternative preliminary configuration designs and was used for that purpose in Ref. 1.

3. System Description

The Ref. 1 mathematical models of the airframe the atmospheric turbulence environment, and the "terrain" (sea surface), are reviewed next. The overall closed loop configuration is shown in Fig. 3.

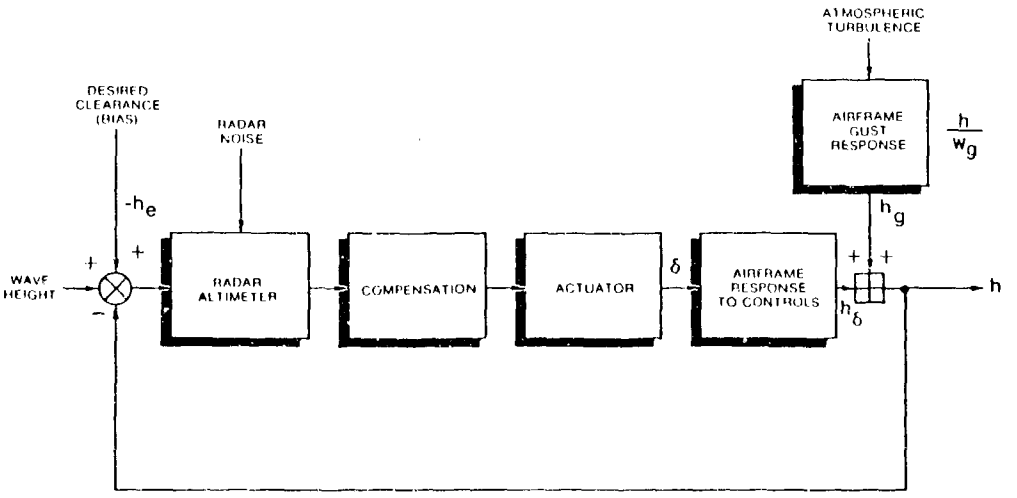

Figure 3. Terrain-Following System Block Diagram

a. Airframe Equations of Motion

Short-period longitudinal equations were employed; it was assumed that airspeed variations were suppressed perfectly by an outer throttle loop. The equations of motion were written in terms of height perturbations (h) and pitch angle perturbations (θ) as:

$$\begin{bmatrix} s-Z_w & -Z_\alpha \\ -M_{\dot{w}}s-M_w & s^2-(M_q+M_{\dot{\alpha}})s-M_\alpha \end{bmatrix} \begin{bmatrix} -sh \\ \theta \end{bmatrix} = \begin{bmatrix} Z_\delta \\ M_\delta \end{bmatrix} \delta + \begin{bmatrix} -Z_w+Z_q s/U_o \\ -M_w+M_q s/U_o-M_{\dot{w}}s \end{bmatrix} w_g \qquad (1)$$

δ denotes a single control surface deflection, and w_g is the vertical component of turbulence. The terms $Z_q s/U_o$, $M_w s/U_o$ multiplying w_g are "gust-gradient" terms. Following customary practice the Z_q term is neglected, since $Z_q \ll U_o$.

The principal transfer functions of interest are those describing the height response to control and also to vertical gust components.

$$\frac{n}{\delta} = \frac{-Z_\delta s^2 + Z_\delta(M_q + M_{\dot{\alpha}})s + Z_\delta M_\delta - M_\delta Z_\alpha}{s^2\left[s^2 - (M_q + M_{\dot{\alpha}} + Z_w)s - M_\alpha + M_q Z_w\right]} \qquad (2)$$

$$\frac{h}{w_g} = \frac{Z_w(s - 2M_q)}{s^2\left[s^2 - (M_q + M_{\dot{\alpha}} + Z_w)s - M_\alpha + M_q Z_w\right]} \qquad (3)$$

b. Sea Spectrum

Reference 1 employed a modified Bretschneider wave spectrum appropriate to a short-crested sea, of Sea State 5, and a 20 knot windspeed. For a missile traversing this sea at M = 0.7, flying into the inertial wind direction, the wave height encountered frequency characteristics are described by the following power spectrum:

$$\phi_{h_w h_w} = \left(\frac{813.9\ \omega_e^2}{(\omega_e^2 + 6.3^2)^2}\right)^2 \qquad (4)$$

where

h_w = Wave height above mean sea level, ft

ω_e = Frequency of encounter, rad/sec

Figure 4 graphs this spectrum. As shown in Ref. 1, it is a good approximation to the exact Bretschneider spectrum, which is described by a more complicated mathematical expression.* Note that it is of relatively narrow bandwidth, with most of the power concentrated in the region 2 to 10.0 rad/sec. This is different from typical land terrain spectra which do not attenuate at low frequencies. The rms wave height is 9.18 ft.

c. Turbulence Spectrum

The well known Dryden spectrum for atmospheric turbulence was employed. For the given flight condition, assuming an rms value of w_g of 2.9 fps this gives:

$$\phi_{w_g w_g} = \frac{(14.0438)^2(\omega^2 + 4.5143)^2}{(\omega^2 + 7.819^2)^2} \tag{5}$$

This spectrum is also shown on Fig. 4.

d. Stability Derivatives

Stability derivatives were calculated in Ref. 1 for each of the configurations 3GA, 6GA, 9GA, 6F, 9F, and 6H shown in Fig. 1. In all cases a positive static margin was assumed as listed in Table 1, which also gives weights and inertias. Table 2 lists the derivatives and the h/δ and h/w_g transfer functions in the forms:

$$\frac{h}{\delta} = \frac{A_{h_\delta} s^2 + B_{h_\delta} s + C_{h_\delta}}{s^2(s^2 + Bs + C)}$$

$$\frac{h}{w_g} = \frac{A_{h_{w_g}} s + B_{h_{w_g}}}{s^2 (s^2 + Bs + C)} \tag{6}$$

*For more background on the Bretschneider wave spectrum see Ref. 2.

TABLE 1. FLIGHT CONDITIONS FOR TERRAIN-FOLLOWING ANALYSIS

Mach No. = 0.7

Altitude = Sea Level

For all configurations

% Total Fuel Used = 50.5%, for Configurations 3GA, 6GA, 9GA, 3F, 6F, 9F

= 6.2%, for Configuration 6H

Configuration	3GA	3F	6GA	6F	6H	9GA	9F
Weight (lb)	2234.9	2077.69	2396.8	2183.52	2771.5	2622.7	2320.58
Pitch Inertia (sl-ft^2)	1620.0	1591.03	1815.6	1644.2	2363.54	1983.5	1789.7
Static Margin (ins.)	4.175	2.012	5.907	1.992	2.0	7.23	2.0562
Reference Area* (ft^2)	11.5	10.0	23.0	20.0	15.9992	34.5	30.0
C_L at 1 g	0.2673	0.2858	0.1434	0.1502	0.238	0.1046	0.1064
g Per Degree of Control Deflection†	1.1341	1.1907	1.5478	3.0099	2.5817	2.8766	4.5531

*The reference area is the area employed to define C_L. For Configurations 3GA, 6GA, 9GA it equals the gross wing area, for Configurations 3F, 6F, 6H, and 9F it equals the gross horizontal projected area of the joined wings (excluding the canard for 6H).

†"Control" = all-moving tail for 3GA, 6GA, 9GA; wing-warping (measured at front wing root) for 3F, 6F, 9F, and all-moving canard only for 6H.

TABLE 2. DERIVATIVES AND TRANSFER FUNCTIONS

(Flight Conditions Specified in Table 1)

	CONFIG. 3GA	CONFIG. 6GA	CONFIG. 9GA	CONFIG. 3F	CONFIG. 6F	CONFIG. 9F	CONFIG. 6H*
MALPHA	-14.30900000	-36.14000000	-60.76000000	-3.97450000	-7.36460000	-10.00340000	-5.24880000
MW	-0.01830000	-0.04620000	-0.07770000	-0.00510000	-0.00940000	-0.01280000	-0.00671200
ZALPHA	-959.8800000	-1,790.900000	-2,345.450000	-588.7485000	-1,003.024900	-1,444.244800	-864.7700000
ZW	-1.22760000	-2.29040000	-3.14040000	-0.75300000	-1.38510000	-1.84710000	-1.10600000
MA DOT	-0.12480000	-0.22230000	-0.29620000	-0.07560000	-0.21080000	-0.41330000	-0.27900000
MW DOT	-0.00015960	-0.00028430	-0.00037880	-0.00009670	-0.00026960	-0.00052850	-0.00035700
MDELTA	0.59050000	1.12900000	1.56460000	0.25000000	0.70510000	1.21540000	0.57070000
ZDELTA	1.81860000	3.81859000	5.60510000	-3.13910000	-6.03610000	-8.43150000	-1.31800000
MQ	-0.40800000	-0.72450000	-0.98000000	-0.25180000	-0.70270000	-1.37750000	-0.69800000
B	1.76040000	3.23720000	4.41660000	1.00040000	2.29860000	3.63790000	2.08300000
C	14.80986000	37.79939480	63.83759200	4.16410540	8.33790977	12.54778025	6.01998800
A, H DELTA	-1.81860000	-3.81859000	-5.60510000	3.13910000	6.03610000	8.43150000	1.31800000
B, H DELTA	-0.96895000	-3.61544101	-7.15322862	1.02774134	5.51397735	15.09913020	1.28768600
C, H DELTA	540.7867926	1,883.922257	3,501.231194	159.6634780	808.0943191	1,839.678797	500.4411030
A, H WG	-1.22760000	-2.29040000	-3.14040000	-0.75300000	-1.38510000	-1.84710000	-1.10600000
B, H WG	-1.00172160	-3.31878960	-6.15518400	-0.37921080	-1.94661954	-5.08876050	-1.54397600

*With canard 1/4-chord sweep angle $\Lambda_{c/4}$ = 35 deg.

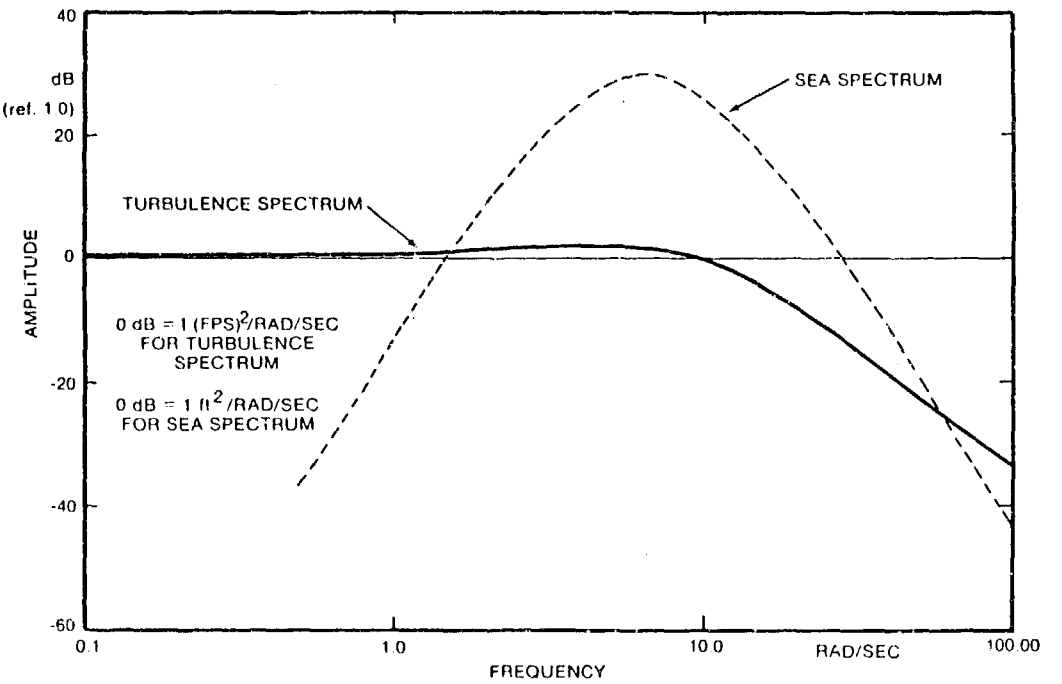

Figure 4. Command and Disturbance Spectra

C. LIMITS ON OPTIMUM TERRAIN-FOLLOWING PERFORMANCE (SINGLE CONTROLLER)

For a given airframe, the guidance system can be designed to minimize $E(h_e^2)$ through the use of optimal control theory. This yields the guidance system that gives the minimum achievable $E(h_e^2)$ for a specified level of mean square control deflection $E(\delta^2)$.

It might be thought that any desired level of $E(h_e^2)$, even zero, could be obtained by allowing $E(\delta^2)$ to increase. This is <u>not</u> true for conventional (aft tail) configurations in which elevator is employed to control height. Such configurations have height-to-elevator transfer functions which incorporate one or more right-half-plane zeros. (Transfer functions of this kind are called "nonminimum phase.") For such a system there is a finite minimum achievable mean square error (Ref. 1).

2. Optimum Single-Controller System

Reference 1 derives the equations for the optimal single-controller system, i.e., the system that minimizes the performance index, J.*

$$J = E(h_e^2) + k^2 E(\delta^2) \tag{7}$$

For a given k^2 we wish to know the value of $E(h_e^2)$ obtained, and the associated mean square control deflection $E(\delta^2)$. As shown in Ref. 1, these values are given by expressions of the type:

$$E(h_e^2)_{opt} = \frac{1}{2\pi j} \int_{-j\infty}^{j\infty} \{W_1 \phi_{RR} \bar{W}_1 + W_2 \phi_{dd} \bar{W}_2\}\, ds \tag{8}$$

$$\text{Associated } E(\delta^2) = \frac{1}{2\pi j} \int_{-j\infty}^{j\infty} \{W_a \phi_{RR} \bar{W}_a + W_b \phi_{dd} \bar{W}_b\}\, ds \tag{9}$$

In each expression the first term gives the contribution to J that stems from the portion of h_e or δ that is correlated with the terrain. The second term gives the contribution due to the portion of h_e or δ that is correlated with the atmospheric turbulence. Only two terms appear in each expression: there are no cross-correlation terms involving ϕ_{Rd}, ϕ_{dR} because it has been assumed that the terrain (waves) and turbulence are uncorrelated.

$E(h_e^2)_{opt}$ and the associated $E(\delta^2)$ were calculated in Ref. 1 for each of the configurations in Fig. 1. The results are presented below.

3. Conventional (Aft Tail) Configurations

Figure 5 shows the mean square height error, $E(h_e^2)$, for aft tail configurations 3GA, 6GA, and 9GA graphed versus the corresponding mean square control deflection $E(\delta^2)$ required by the optimal control system.

---

*See Refs. 4 and 5 for additional details on the theoretical development.

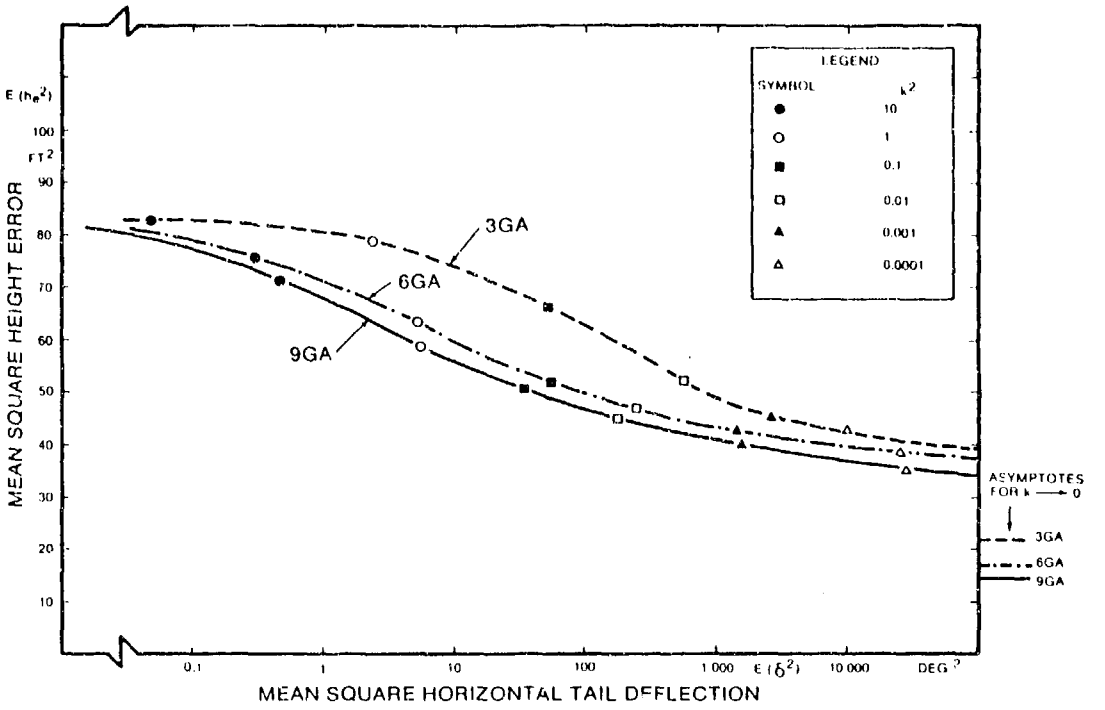

Figure 5. Optimal Terrain-Following Performance of Single-Controller Aft Tail Configurations

Values of the weighting parameter k are indicated on the graphs. (The control deflection, δ, indicates deflection of the all-moving tail surfaces in units of degrees.) At high values of k (i.e., "expensive control") corresponding to the left side of the graphs the control deflections are small and have little effect on the missile, which flies more or less in a straight line with the preponderant part of the height error being due to the waves. Thus the asymptote of $E(h_e^2)$ for $k \to \infty$ is essentially equal to the mean square wave height, 81.2 ft^2. As k is decreased the system accuracy increases, but for reasonable values of $E(\delta^2)$, e.g., of the order of 10 deg^2, the gain in accuracy is slight. For example, with $E(\delta^2) = 10$ deg^2 Configuration 3GA reduces its mean square error only to 74/81.2 = 0.91 of its open-loop value. If much larger $E(\delta^2)$ could be produced or if the control effectiveness parameters C_{L_δ}, C_{M_δ}, could be increased the accuracy could be improved, but even with infinite mean square control deflections the best accuracy that can be achieved with airframe 3GA is only $E(h_e^2) = 22$ ft^2, i.e., 0.27 of the open-loop mean square error.

This situation is only slightly improved by selecting a larger wing area, as shown by the graphs for Configurations 6GA and 9GA in Fig. 7. Nor is any significant improvement gained by reducing static margin. This expedient was studied by recalculating the optimum system performance with M_α set equal to zero, and the remaining derivatives unchanged. For any given k the zero static margin values of $E(h_e^2)$ and $E(\delta^2)$ were, when graphed on Fig. 5, virtually coincident with the points graphed for the normal static margins listed in Table 1.

It is clear from the above results that, even with ideal guidance system dynamics (e.g., no actuator lags, no digital processing delays), the mean square control deflections required for close terrain-following of the assumed wave spectrum are prohibitively large for the aft tail configurations.

4. Atmospheric Turbulence Response

The Dryden spectrum employed to describe low altitude turbulence (Eq. 5) is widely employed in aircraft guidance and control studies. The mean square height error due to turbulence was much smaller than that due to terrain for all the configurations studied. Therefore the effect of varying the Dryden spectrum is secondary, hence no parametric variations of atmospheric turbulence characteristics were performed in Ref. 1, or in the present study.

5. Terrain-Following Performance of Single-Controller Joined Wing Configuration

The joined wing configurations 3F, 6F, 9F obtain pitch control via wing-warping, as described in Section 3 of Ref. 1. With a parabolic variation of twist, corresponding to uniform torsional modulus GJ along both wings, the center of pressure of the lift induced by twist is ahead of the c.g., and hence the height/twist transfer function is minimum phase. However, the pitching moment arm is small for Configuration 3F. For the hybrid configuration, 6H (Fig. 3c), a long moment arm is obtained by employing an all-moving canard as the primary pitch control.

Figures 6 and 7 shows the terrain-following performance of these configurations when optimally controlled. The gust and wave spectra are identical to those employed previously. Comparing Figs. 6 and 7 with Fig. 5 it is seen that the joined wing and hybrid configurations yield a mean square height error which tends to zero as $k \to 0$. Unfortunately, as was the case with the aft tail configuration, the magnitudes of the control deflection $E(\delta^2)$ are impractically large for close terrain-following of the assumed short-crested sea. The reason for this is explained below.

Consider Eq. 10, which gives the h/δ transfer function for Configuration 6H, where δ = deflection of the all-moving canard, measured in degrees:

$$\frac{h}{\delta} = \frac{1.318s + 1.287687s + 500.441103}{s^2(s^2 + 2.083s + 6.019988)} \tag{10}$$

or

$$\frac{h}{\delta} = \frac{1.318(s + 0.4885 \pm 19.4797j)}{s^2(s^2 + 2.083s + 6.019988)} \tag{11}$$

The Bode diagram of Eq. 10, given on Fig. 8, exhibits a pronounced dip around 19.5 rad/sec, due to the light damping of the numerator factors. This dip attenuates the h/δ response in the region where it is most needed, i.e., in the region around the peak of the wave spectrum. If the dip is eliminated (or smoothed) the response improves dramatically. This can be demonstrated by calculating the mean square height error and mean square control deflections for a smoothed transfer function:

$$\frac{h}{\delta} = \frac{100}{s^2} \tag{12}$$

yielding $E(h_e^2) = 45.1\ ft^2$ and $E(\delta^2) = 6.8\ deg^2$.

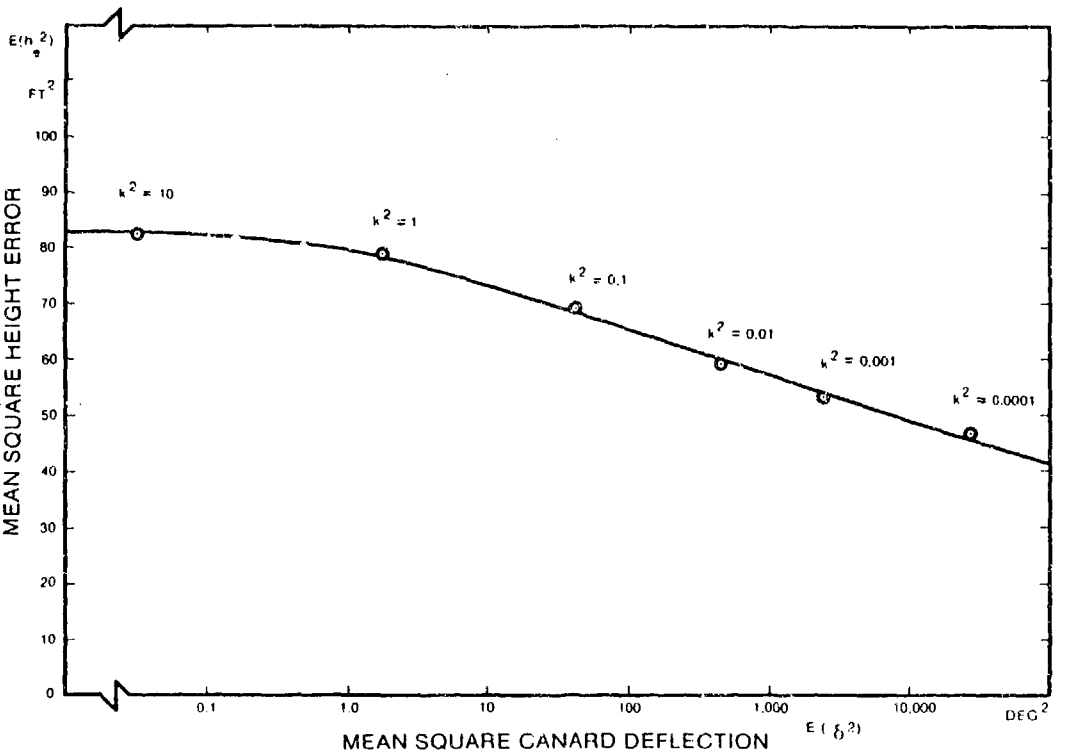

Figure 6. Optimal Terrain-Following Performance; Hybrid Configuration

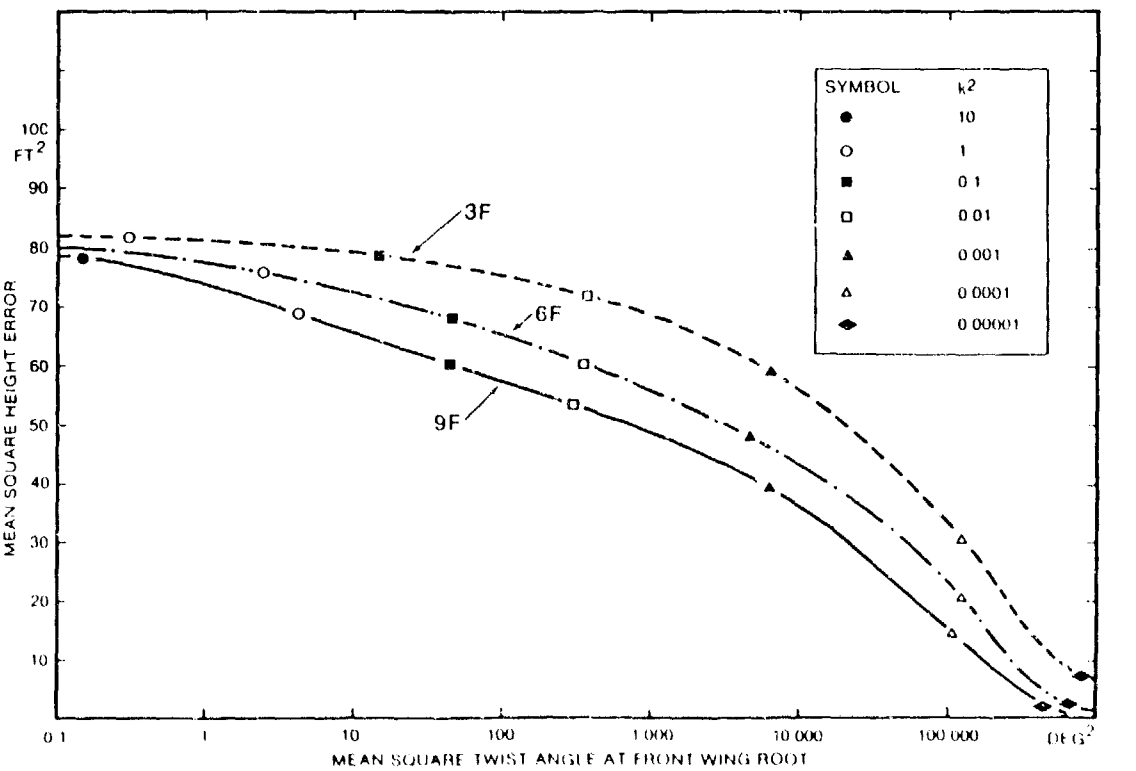

Figure 7. Optimal Terrain-Following Performance; Joined-Wing Configurations

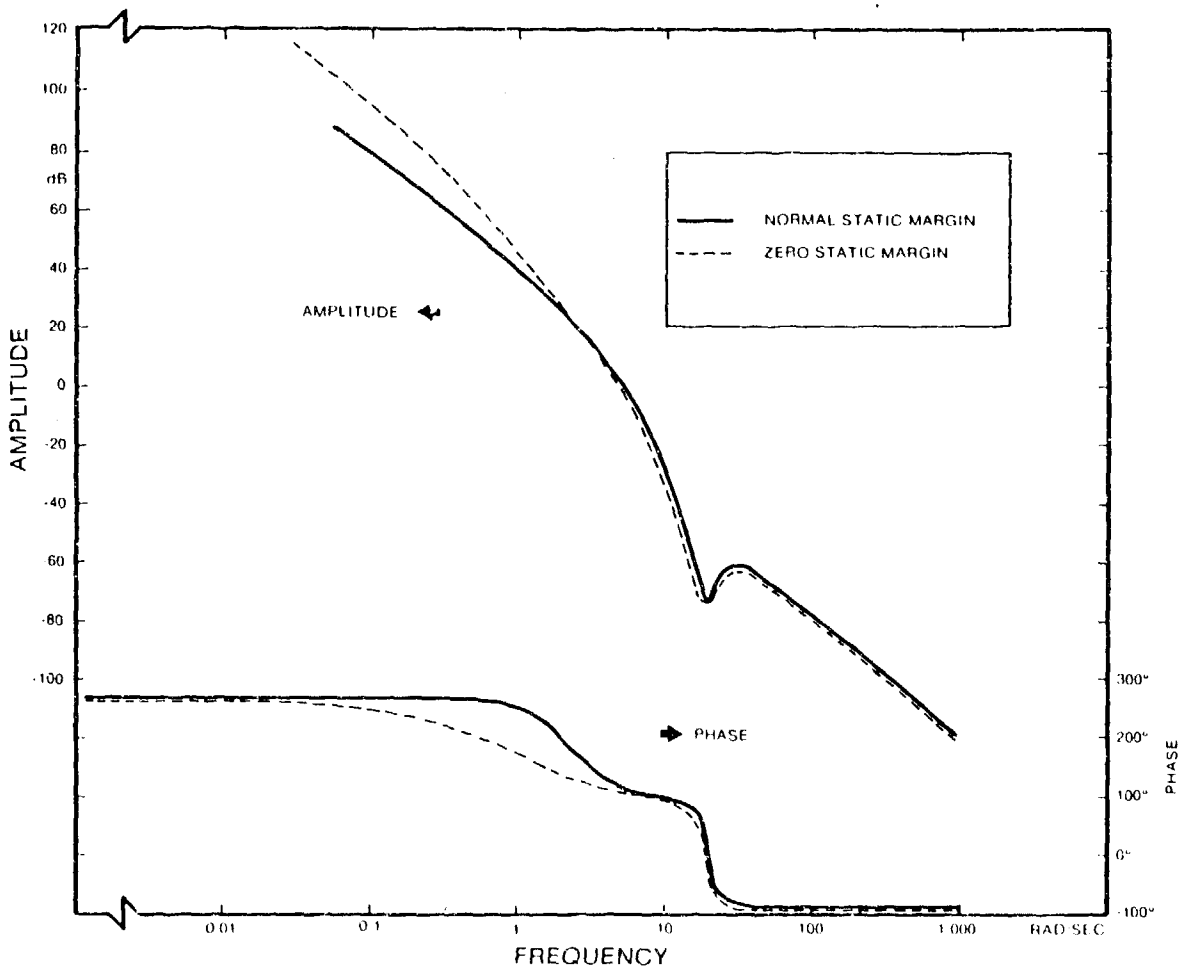

Figure 8. Height/Canard Deflection Transfer Functions for Hybrid Configurations

The results presented up to this point of the present report were previously given in Ref. 1. That reference is primarily concerned with airframe-centered aspects of Cruise Missile Design, and does not investigate the practical realizability of the Theoretical Optimum Guidance Systems. By contrast, the present report is not solely concerned with the optimum level of performance, but also addresses the question of whether the optimum compensation can be constructed from practical components. The next section shows that, although the theoretical optimum compensation cannot be achieved in practice, it can be closely approximated, with negligible performance penalty being induced by the approximation.

SECTION III

COMPENSATION NETWORK

A. INTRODUCTION

The compensation network required by the optimal controller is shown to require ideal lead. The governing equations, described in Appendix A of Ref. 1, are first reviewed.

B. SIMPLIFIED SYSTEM MODEL

A simplified model, which ignores the gust disturbance input, is given in Fig. 9. R represents the "sea input", G_c is the compensation network and G represents the open loop dynamics of h/δ. From Fig. 9, write

$$\delta = [1 + G_c G]^{-1} G_c R = W_a R \tag{16}$$

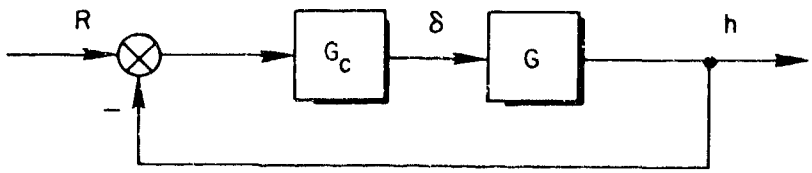

Figure 9. Simplified System Model

and recall that W_a represents the quantity to be determined in the optimization process. Specifically, the Wiener-Hopf equation of interest is

$$\left[1 + \frac{1}{k^2} G\bar{G}\right] W_a \phi_{RR} - \frac{\bar{G}}{k^2} \phi_{RR} = \psi \tag{17}$$

For the modified Bretschneider spectrum, the solution is obtained by letting G = N/D where N is 2nd order, D is fourth order)

$$W_a = \frac{D}{\Delta}\left[\frac{\bar{N}}{\bar{\Delta}k^2}\frac{s^2}{(s+6.3)^4}\right]_+ \frac{(s+6.3)^4}{s^2} \tag{18}$$

D represents the open loop roots and Δ represents the optimal closed loops. From Appendix A, Ref. 1,

$$\frac{\bar{N}s^2}{\bar{\Delta}(s+6.3)^4} = \frac{L_a}{(s+6.3)^4} \tag{19}$$

where L_a is a cubic polynomial. Therefore:

$$W_a = \frac{DL_a}{k^2\Delta s^2} \tag{20}$$

For the assumed cruise missile, W_a is 7th order over 6th order.

Next, solve

$$W_a = \left[1 + G_cG\right]^{-1}G \tag{21}$$

for Gc:

$$G_c = W_a\left[1 - GW_a\right]^{-1} = \frac{1}{k^2}\frac{DL_a}{(\Delta s^2 - NL_a)} \tag{22}$$

We see that the numerator of G_c in 7th order while the denominator is 6th order, indicating pure lead at high frequency. The practical significance of this requirement can be assessed by considering the Bode diagrams of G_c for two typical examples, as discussed below.

C. SPECIFIC EXAMPLES

The Bode plots for G_c, are shown in Figs. 10 and 11 for the aft-tail Configuration 9F and the joined wing plus canard Configuration 6H, respectively. Each G_c is stable, as determined by a Routh-Hurwitz Test, i.e. all the poles lie in the left-half-plane.

Within the frequency region $1 < \omega < 50$ rad/sec the Bode diagrams can be closely approximated by Bode diagrams of systems without pure lead, i.e., systems having transfer function numerators of equal or lower order than the corresponding denominators. Outside this frequency region the amplitude of the wave spectrum is small, hence the practical inability to generate the pure lead demanded by the optimum G_c is not important. Note also that for $\omega > 50$ rad/sec an accurate solution requires a more complex airframe and control system model than considered here. Such a model would include actuator lags, digital processing lags and aeroelastic modes. If such high-frequency effects were included the optimum G_c would change. Nevertheless it would always be possible to avoid G_c having a higher order numerator than denominator by appropriate adjustment to the high frequency characteristics of the wave spectrum. Such adjustment would involve a negligible loss of performance.

From the above discussion we reach the following conclusions regarding the optimum compensation:

1) It is stable.

2) It cannot be physically realized exactly, due to the requirement for a pure lead (i.e., an ideal differentiator).

3) It can be closely approximated by a physically realizable compensation with negligible loss of performance.

D. SECTION SUMMARY

The optimal compensation is a ratio of polynomials in the complex frequency variables. The numerator is seventh order whereas the denominator is sixth order, indicating the need for approximation of the

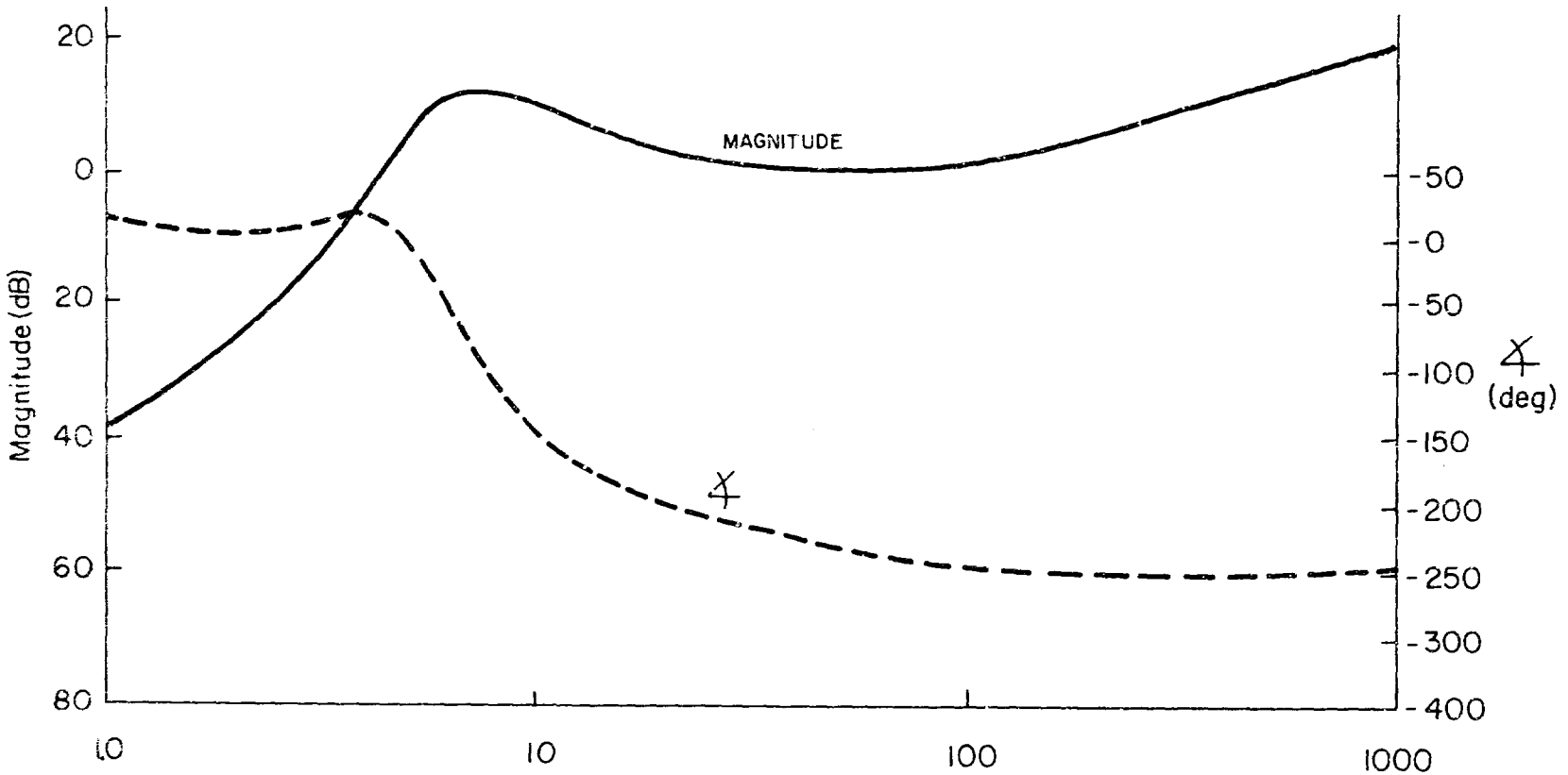

Figure 10. Compensation for 9F Configuration

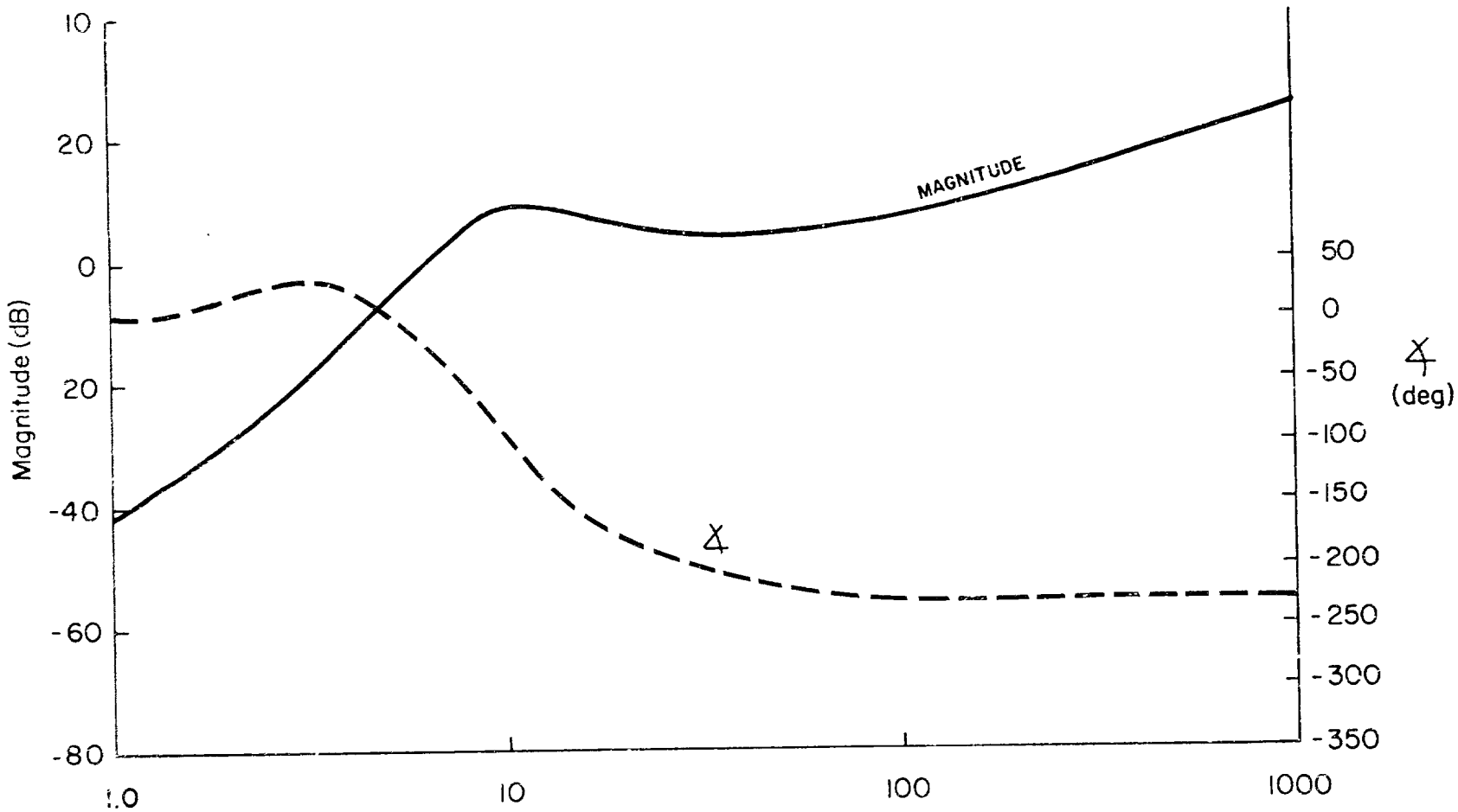

Figure 11. Compensation for 6H Configuration

optimal compensation at high frequencies. Bode plots for the compensation networks were given for the 9F and 6H configurations. Each network is stable.

SECTION IV

EFFECT OF ALTERNATIVE TERRAIN

A. INTRODUCTION

A short-crested sea spectrum was selected as the "terrain" to be followed in the examples presented in the previous sections. It is clear from Figs. 5, 6 and 7 that, even for optimal systems, this terrain is hard to follow. Large control deflections are required to obtain close terrain-following. For the nonminimum phase (conventional wing-plus-tail) configurations, even infinitely large control deflections cannot reduce the mean square height error, $E(h^2)$, much below 20 ft^2, i.e., approximately 25 percent of the open-loop mean square error. In this section we examine the effect of alternative terrain spectra. Reference 1 briefly discussed the asymptotic behavior of the nonminimum phase airframes following various types of terrain, i.e., their behavior with unlimited control deflections. Reference 1 did not study how the accuracy of terrain-following obtainable with finite control deflections is affected by the terrain spectrum. This important question is addressed below.

B. ALTERNATIVE TERRAIN SPECTRA

Various land terrain spectra are in use (see Ref. 3). The simplest of these is the first-order form:

$$(\phi_{RR})^+ = \frac{\sqrt{2a[E(R)^2]}}{s + a} \tag{23}$$

In this equation $E(R^2)$ is the mean square terrain altitude variation and a is the encounter break frequency, which depends on the terrain roughness and missile speed as follows:

$$a = \frac{V_I}{a_s} \tag{24}$$

where

V_I = Missile Inertial Speed (FPS)

a_s = Spatial Correlation Distance (FT), i.e., the average distance between two sample terrain points which differ in magnitude by a factor of 1/e = 0.368.

Here we shall consider two types of terrain:

1) Rolling terrain with a_s = 2,000 ft

2) Rough terrain with a_s = 500 ft

For both terrains the mean square height variation was chosen as 81.2 ft^2. This value equals the mean square wave height variation of the wave spectrum analysed in previous sections. It is a convenient choice because it removes the effect of terrain amplitude when making comparisons between the results to be presented in this section and those given in earlier sections. Since the optimum system is linear, the results may, of course, be scaled for any terrain amplitude of interest. The terrain spectra then become:

For Rough Terrain

$$(\phi_{RR})^+ = \frac{15.932}{s + 1.563} \tag{25}$$

For Rolling Terrain

$$(\phi_{RR})^+ = \frac{7.9584}{s + 0.39} \tag{26}$$

C. TERRAIN-FOLLOWING PERFORMANCE

Figure 12 presents the results of Wiener-Hopf optimizations for Configurations 6GA and GF, following rolling terrain. The abscissa is the expected value of the mean square control deflection $E(\delta^2)$. Care must be used in interpreting $E(\delta^2)$ since the control surfaces employed for the joined wing Configuration 6F are different from those used in the conventional Configuration 6GA. For Configuration 6F δ denotes the

number of degrees of wing warp applied at the wing root. A reasonable limiting value based on maximum "g" structural limits for Configuration 6F is $-15 < \delta < 15$ degrees. For Configuration 6GA δ denotes the deflection of the horizontal tail, measured in degrees. Typically, for similar maximum "g" this δ would be in the range $-5 < \delta < 5$ degrees. Thus, reasonable maximum levels of $E(\delta^2)$ would be 100 deg^2 for Configuration 6F and and 11 deg^2 for Configuration 6GA. The corresponding levels of terrain-following accuracy are $E(h_e)^2 = 17$ ft^2 for 6GA and $E(h_e^2) = 11.8$ ft^2 for Configuration 6F.

Comparing Figs. 5, 6, and 12 shows that the rolling terrain can be followed much more closely than the short-crested sea, for a given mean square control deflection. In particular, for low values of $E(\delta^2)$ of the order of 1 deg, the rolling terrain permits a substantial improvement over open-loop constant-altitude flight, whereas for the short-crested sea only a slight improvement is obtained. As shown in Fig. 13, for rough terrain the results are intermediate between the results obtained for waves and for rolling terrain.

The optimum terrain-following performance of the larger cruise missiles (Configurations 9GA and 9F) is shown in Figs. 14 and 15. The smaller configurations (3GA and 3F) yield optimum $E(h_e^2)$ and $E(\delta^2)$ as illustrated in Figs. 16 and 17. Different definitions of δ for the joined wing, hybrid and conventional configurations makes it difficult to perform meaningful comparisons between the configurations. Nevertheless, it is clear that, if adequate control power is available, the minimum phase Configurations 3F, 6F, 9F, 6H have superior performance.

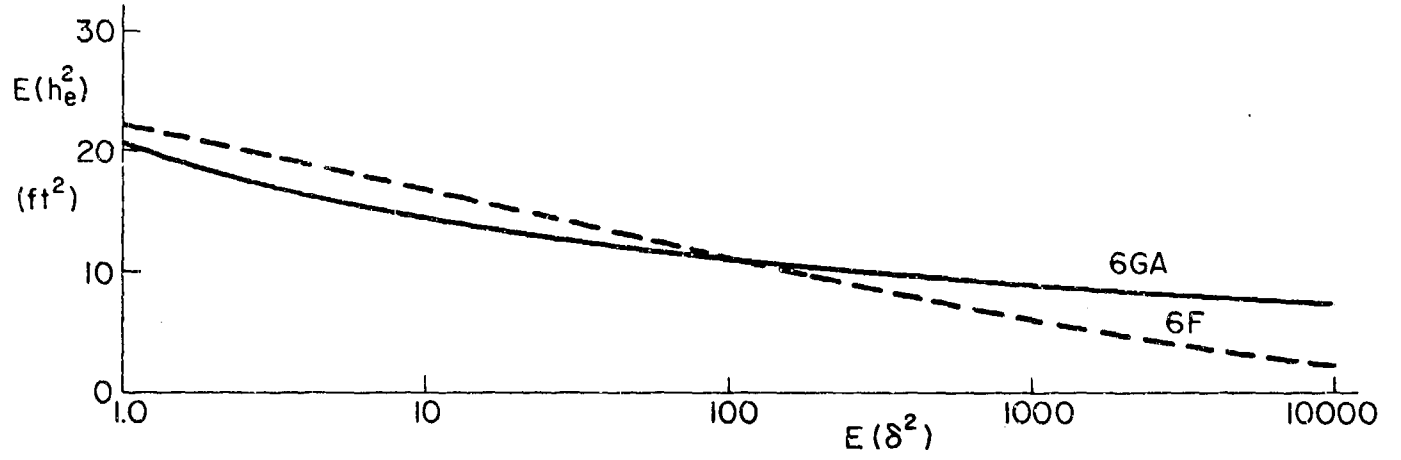

Figure 12. Rolling Terrain; 6GA, 6F

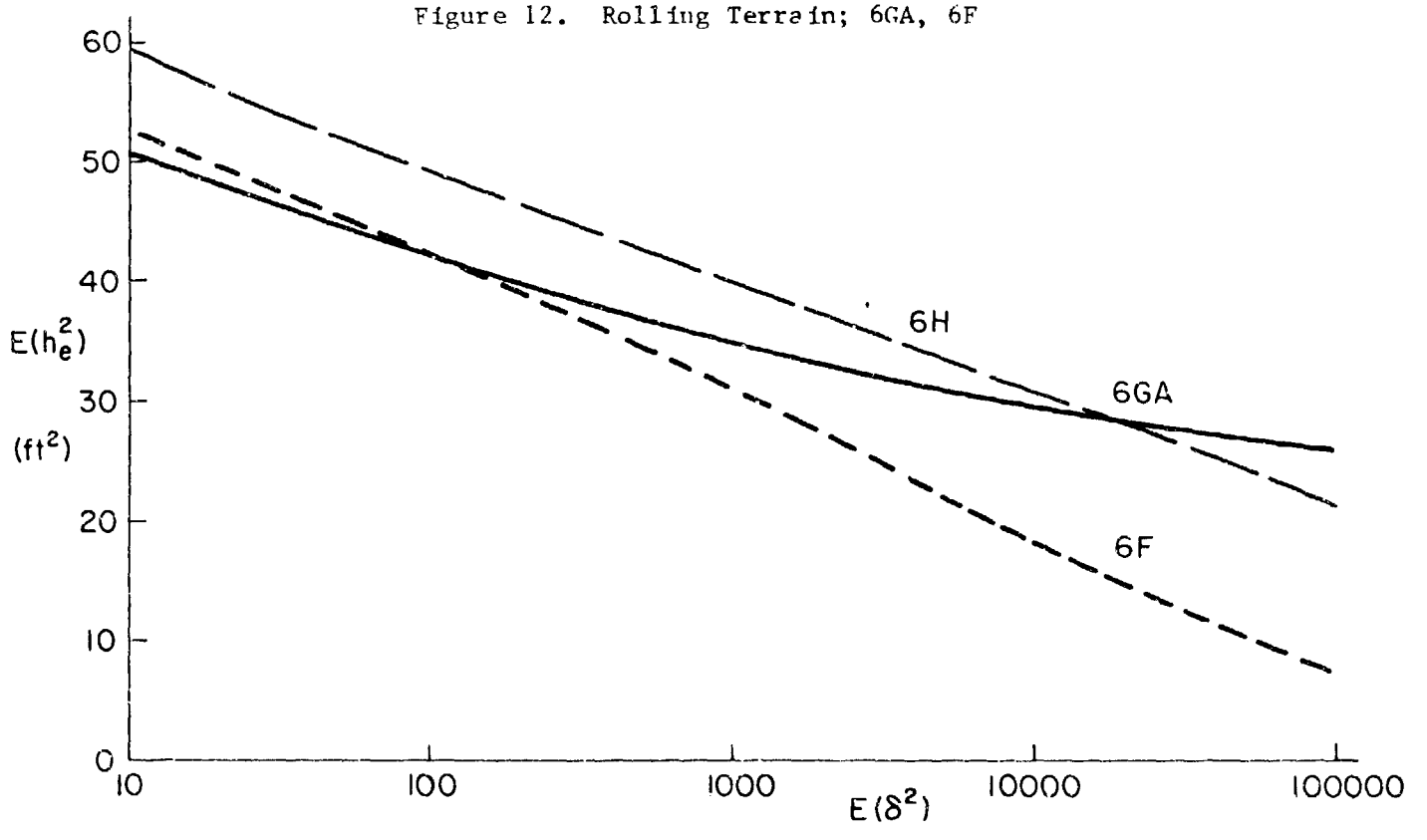

Figure 13. Rough Terrain; 6GA, 6F, 6H

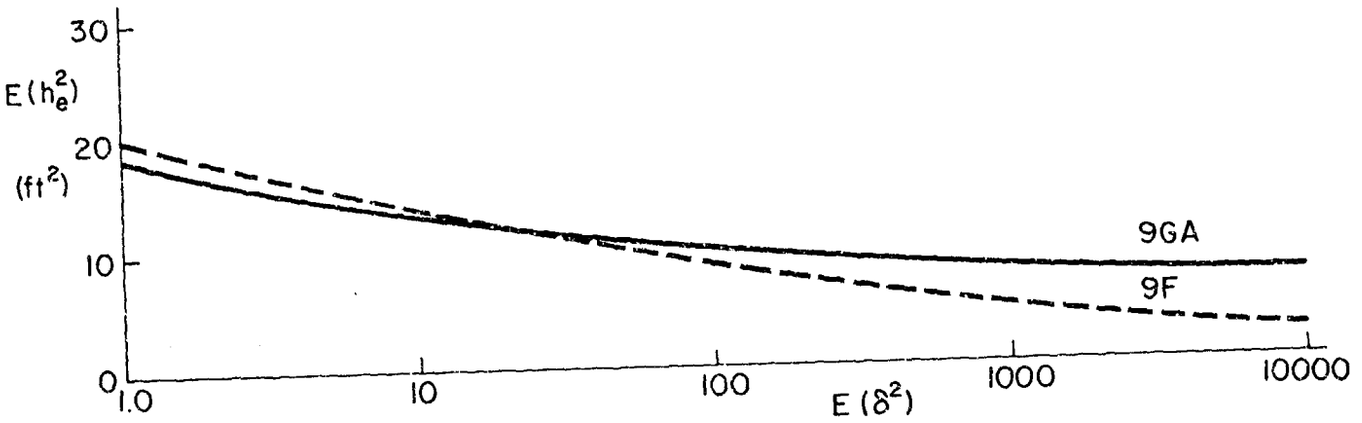

Figure 14. Rolling Terrain; 9GA, 9F

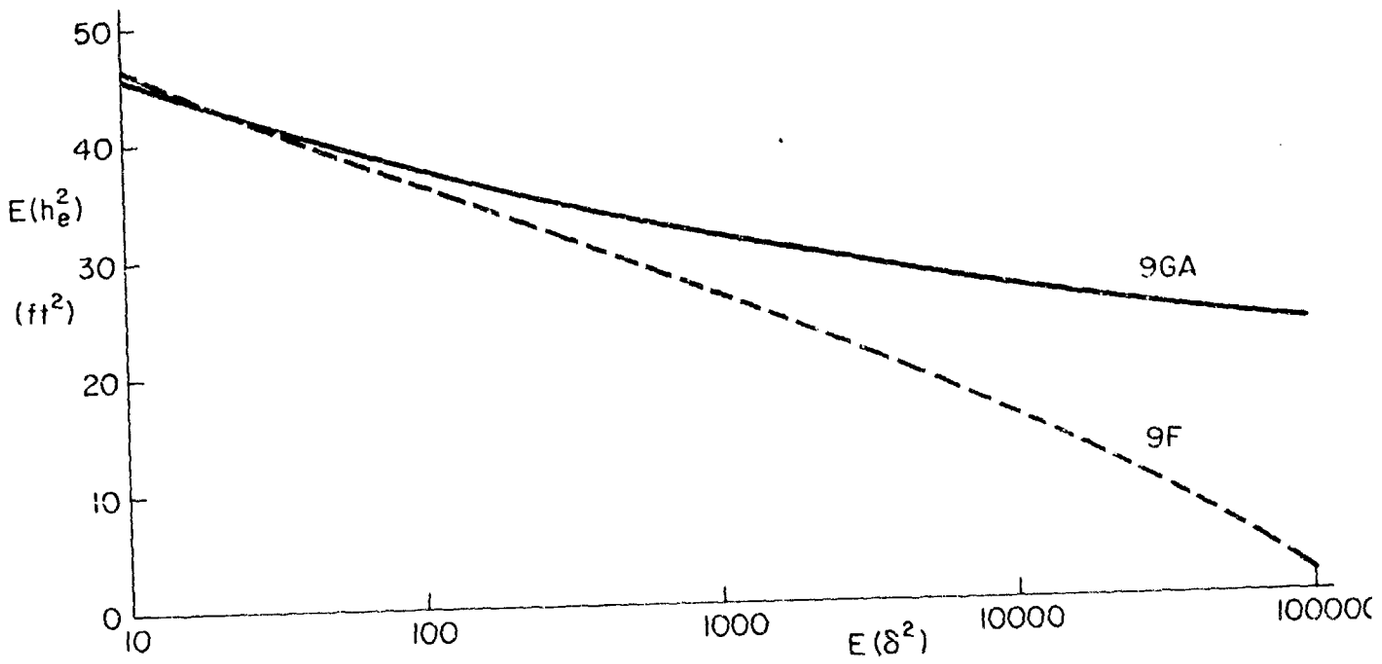

Figure 15. Rough Terrain; 9GA, 9F

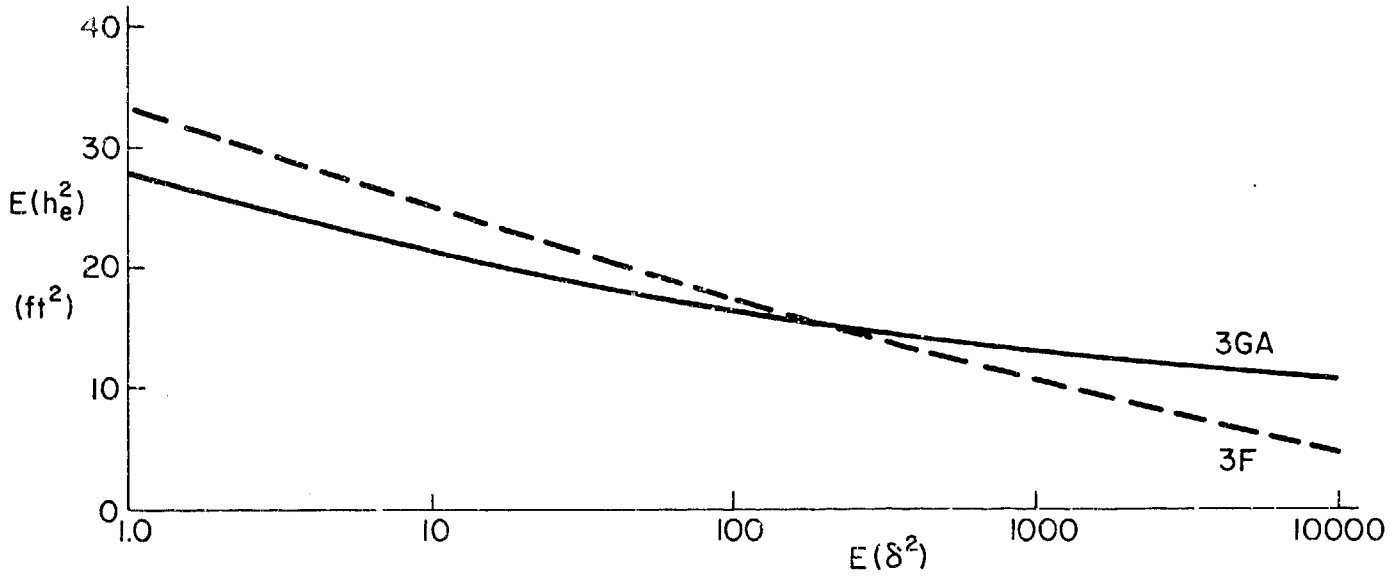

Figure 16. Rolling Terrain; 3GA, 3F

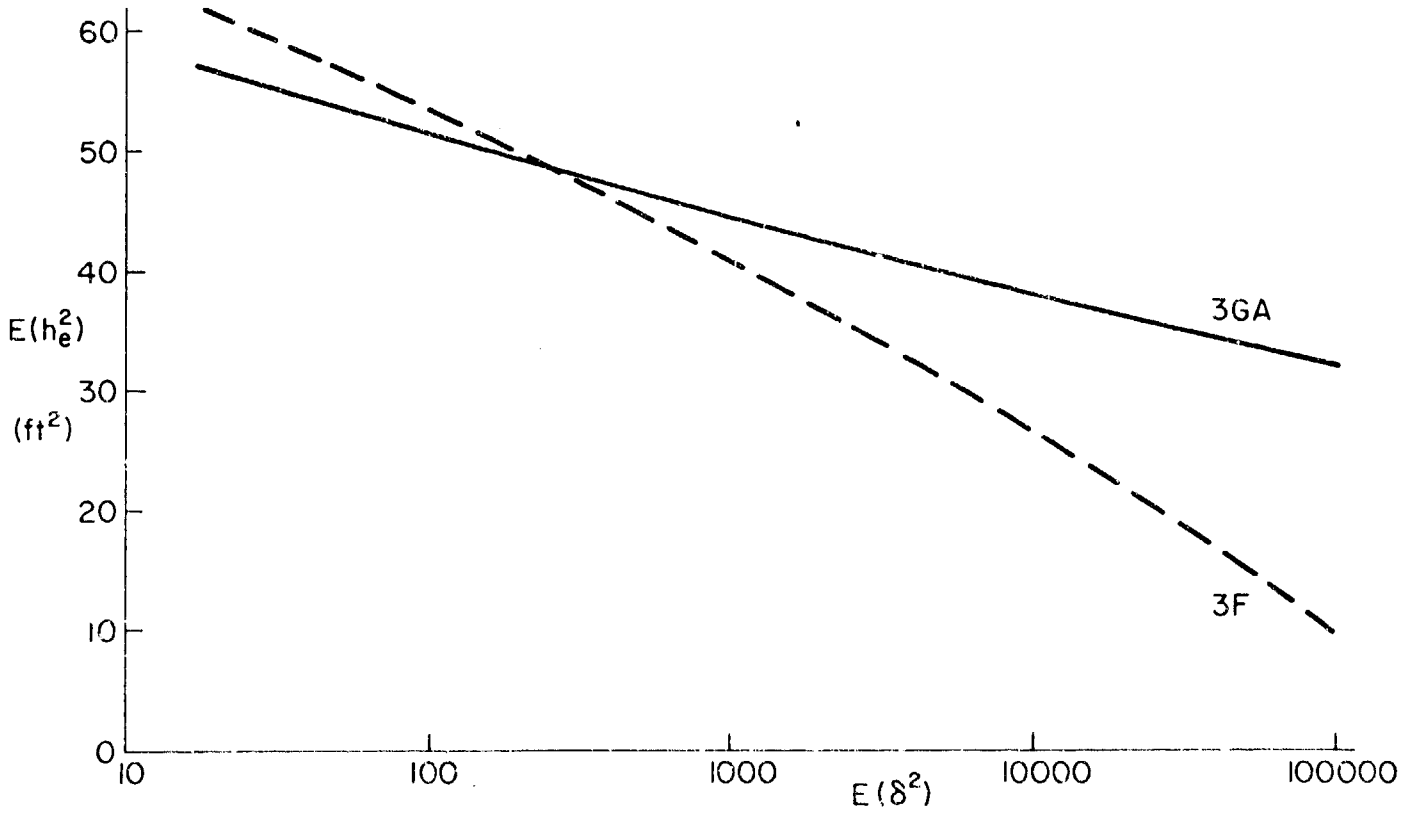

Figure 17. Rough Terrain; 3GA, 3F

SECTION V

COMPARISON OF OPTIMAL AND CONVENTIONAL CONTROL SYSTEM PERFORMANCE

A. INTRODUCTION

Section II of this report has shown that none of the optimally controlled configurations considered achieved close following of the short-crested sea without large control deflections. By definition, the optimal control system yields a smaller $E(h_e^2)$ than any other system. It is therefore of interest to compare the optimal system performance as given in Figs. 5, 6 and 7 with the performance of conventionally designed control systems, i.e., systems which are designed by standard systems synthesis procedures (as opposed to optimal control theory). Our objective is to determine how much is gained by employing an optimal instead of a conventional guidance system.

For simplicity, instead of the exact airframe transfer functions given in Section II we shall assume that the h/δ transfer function is of the form $100/s^2$. This is a reasonable approximation to the exact transfer functions except that it omits the Bode amplitude "dip" around 20 rad/sec. As shown in Section II, elimination of this dip improves the performance of the optimally controlled system, yielding $E(h_e^2) = 6.8\ deg^2$ with $h/\delta = 100/s^2$. These numbers should be borne in mind when reading the results presented below.

Two "Conventional" designs will be studied: first, a washout compensator, second an ideal lead. The former can be physically realized exactly, the latter only approximately, so the results given for the ideal lead compensation are slightly optimistic, but nevertheless approximately indicate the level of performance that could be attained by a conventional system.

B. WASHOUT COMPENSATOR

Consider a washout network in the feedforward path, as defined by Fig. 18. In Fig. 18, R represents the terrain input, E is the attitude error and h is the altitude. Table 3 tabulates $E(\delta^2)$, $E(h^2)$ and $\Delta(s)$ for the closed loop system, and Fig. 19 graphs $E(h^2)$ versus $E(\delta^2)$.

Figure 19 shows that the use of a washout network leads to a peak in the plot of $E(h^2)$ vs. $E(\delta^2)$.

Table 4 compares the washout design against an optimally controlled system with the same transfer function ($100/s^2$).

The results given on Table 3 (and Table 4) assume a $\Delta(s)$ representative of optimally designed systems, i.e., critically damped. For a pole assignment of $\Delta = (s+3)^2 + (5)^2$, an underdamped set, the overshoot is higher; $E(\delta)^2 = 9.75\ \text{deg}^2$, $E(h^2) = 130\ \text{ft}^2$. It is clear that the washout compensated conventional design is considerably inferior to the optimally designed system.

C. IDEAL LEAD COMPENSATION

It was shown in Section III that the optimal design requires lead compensation. Therefore, it is worth checking effects of an ideal differentiator as a compensator for a conventional design (refer to Fig. 20). The values of $E(h^2)$ and $E(\delta^2)$, as well as $\Delta(s)$, the closed loop poles, are tabulated in Table 5 and graphed in Fig. 21. It can be seen that the plot of $E(h^2)$ vs. $E(\delta^2)$ monotonically decreases as $E(\delta^2)$ increases. This is apparently a property of lead compensation. By way of comparison, the optimal system requires 2,528 deg^2 of mean

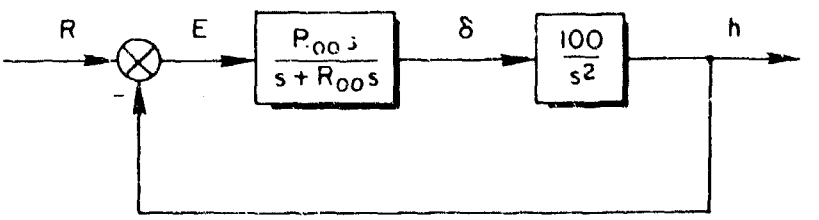

Figure 18. Washout Compensation Feedback System

TABLE 3. CONVENTIONAL DESIGN USING WASHOUT

$E(\delta^2)$	$E(h^2)$	Δ
0.0000033	83.89	$(s+0.2)^2 + (0.1)^2$
0.03328	91.135	$(s+1)^2 + (1)^2$
0.505	104.	$(s+2)^2 + (2)^2$
2.288	112.1	$(s+3)^2 + (3)^2$
6.622	112.85	$(s+4)^2 + (4)^2$
12.787	108.	$(s+5)^2 + (5)^2$
83.524	69.315	$(s+10)^2 + (10)^2$
331.0523	28.3	$(s+20)^2 + (20)^2$
628.915	14.6	$(s+30)^2 + (30)^2$
1593.543	4.17	$(s+60)^2 + (60)^2$
3750.38	1.01	$(s+125)^2+(125)^2$

TABLE 4. COMPARISON OF OPTIMAL DESIGN WITH WASHOUT

DESIGN	$E(\delta^2)$	$E(h^2)$	Δ
Optimal	0.0369	74.9	$(s+2.24)^2 + (2.24)^2$
Washout	0.7774	106.73	$(s+2.24)^2 + (2.24)^2$
Optimal	1.475	54.5	$(s+5)^2 + (5)^2$
Washout	12.787	108.0	$(s+5)^2 + (5)^2$

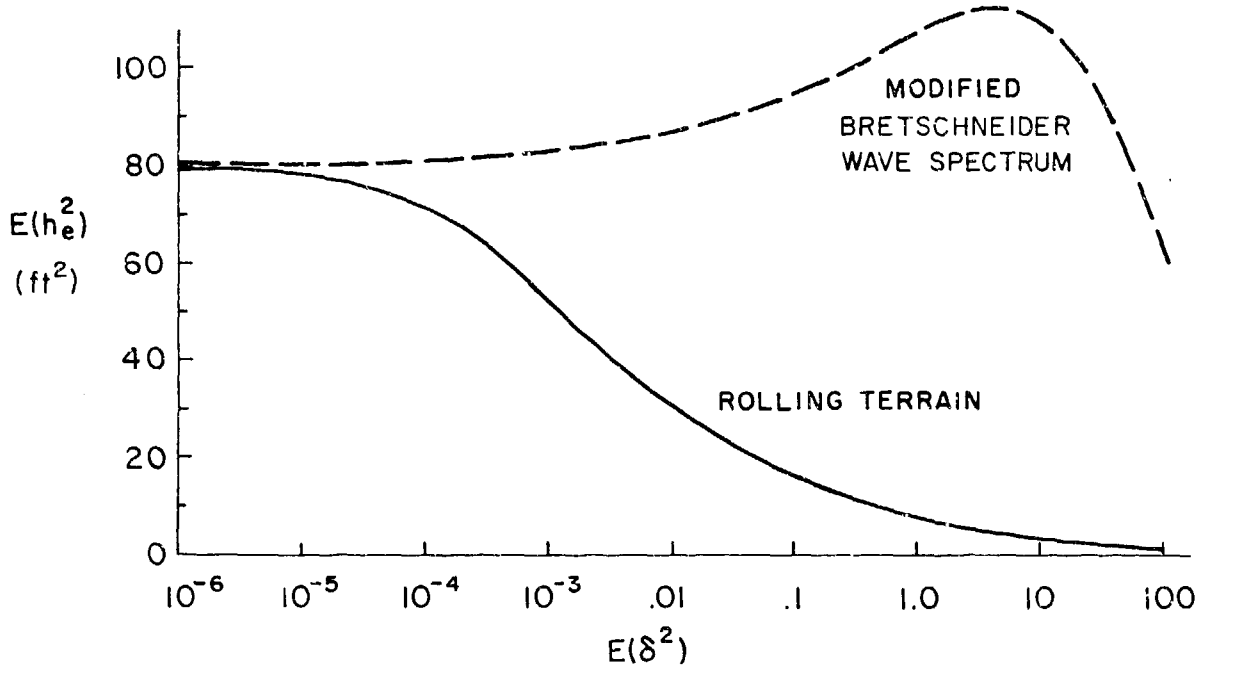

Figure 19. Washout Compensation

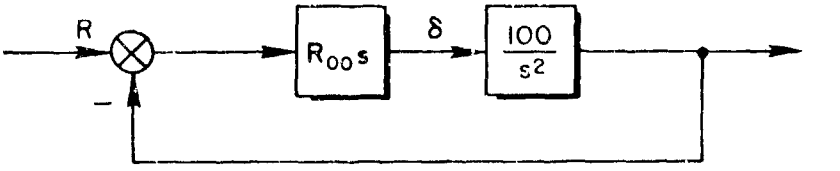

Figure 20. Ideal Lead Compensation

TABLE 5. IDEAL LEAD COMPENSATION

$E(\delta^2)$	$E(h^2)$	Δ
0.0166	83.8	s + 0.01
6.529	77.16	s + 2
37.873	59.304	s + 5
129.01	37.3	(s + 10)
2939.12	1.37	(s + 100)
3791.73	0.9	(s + 125.7)

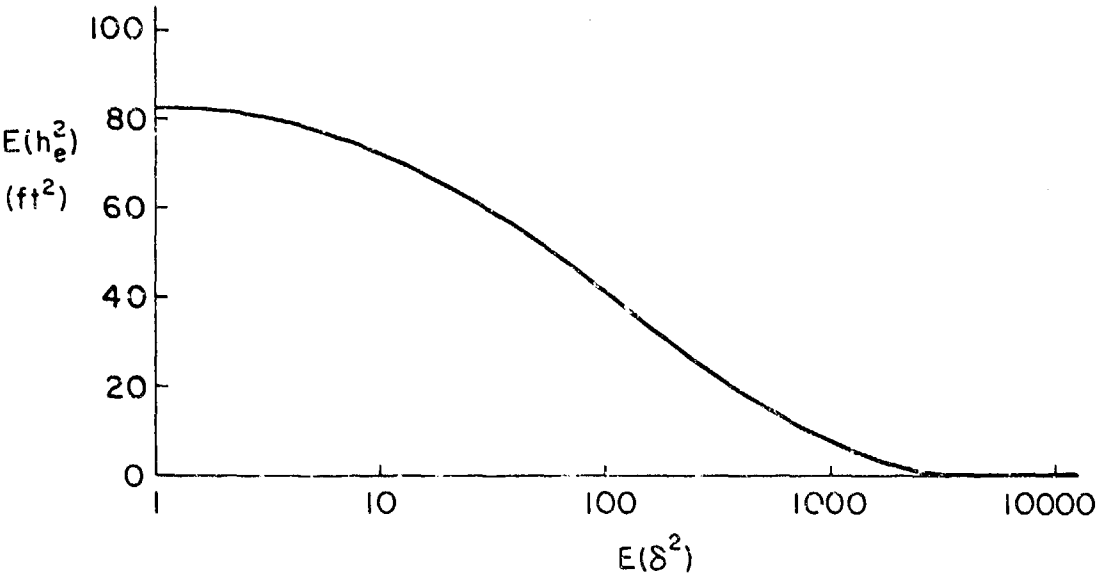

Figure 21. System Performance with Modified Bretschneider, Rolling Terrain, and Pure Lead Compensation

square control deflection to produce 0.9 ft^2 of $E(h^2)$. The "pure lead" "conventional design requires 3,791.73 deg^2. Again, the evidence is clear; the short-crested sea described by the modified Brentschneider spectrum is hard to follow at M = 0.7, even with ideal lead compensation, and such compensation requires larger control deflections than are required by the optimal system.

A physical explanation of the peak in the plot of $E(h^2)$ vs. $E(\delta^2)$ for the conventional design is readily apparent. For $E(\delta^2) = 0$ the controller is in a mode where it follows an inertial altitude reference. For small values of $E(\delta^2)$, with no lead, the vehicle responds out of phase with the input (loop delay is too large) and $E(h^2)$ actually rises above that for following an inertial reference. As $E(\delta^2)$ increases, the bandwidth of the closed-loop system becomes sufficiently wide so that $E(h^2)$ drops below the inertial reference value.

In this regard (see Table 3) note that the bandwidth of the conventional design, for a given $E(h_e^2)$, is much larger than the optimal design. For example, for a $E(h_e^2)$ on the order of 70 ft^2 the bandwidth

of the washout design is of the order of 10 rad/sec, whereas the optimal design's bandwidth is only 2 rad/sec.

The tendency for the plot of $E(h_e^2)$ vs. $E(\delta^2)$ to peak is greatly diminished if, instead of the short-crested sea spectrum, the spectrum for rolling terrain is employed. Figure 19 compares $E(h_e^2)$, $E(\delta^2)$ for the two spectra. This confirms that the peaking occurs because of the added phase lag incurred when no lead compensation is used.

D. SUMMARY

Conventional compensation produces a peak in the plot of $E(h^2)$ vs. $E(\delta^2)$. Lead compensation produces a monotonically decreasing relationship. The performance of the two conventional designs is notably inferior to the system designed by optimal control theory.

SECTION VI

SYSTEM SURVEYS FOR MULTICONTROLLER SYSTEMS

A. INTRODUCTION

The term "Multicontroller" will be used here to denote systems employing two or more separate controls, e.g., flaps plus elevator. In Ref. 1 it was suggested that good terrain-following performance could be obtained by controlling an "inner loop" by means of flaps such that the effective "outer loop" transfer function controlled by the elevator had a desirable form (e.g., K/s^2) for which the h/δ Bode diagram did not have a notch near the wave spectrum peak frequency. Reference 1 did not explore this possibility in detail, although some discussion was given of how a height/elevator transfer function of the form $100/s^2$ could be achieved by employing flaps on Configurations 6H and 6GA. It was concluded that the hybrid Configuration 6H could readily attain the desired inner-loop transfer function, whereas this was more difficult for the conventional 6GA configuration.

Although a multicontroller system can offer improved performance over a single-controller system, the former is necessarily more complex, perhaps prohibitively so for cruise missiles which must satisfy severe constraints on cost and complexity. The decision as to whether or not to employ a multicontroller system therefore depends on whether it can provide a considerable increase in terrain-following accuracy. This question is studied below. The performance of optimally controlled systems with h/δ transfer functions of various forms is assessed, and desirable forms are indicated. The results of this section are of value in deciding whether the additional cost and complexity of a multicontroller system is justified by the increased performance that it provides.

B. SURVEY OF K/s

The mean square height errors and mean square control deflections for K/s open-loop dynamics and the short-crested sea spectrum are

tabulated in Table 6. Also listed is the closed-loop optimal pole. From Table 6 is is seen that an open-loop system with K/s dynamics can produce a small mean square height error (about 10 deg^2 of control deflection with about 3 ft^2 error). Moreover, the closed-loop bandwidth of 30 rad/sec constitutes a reasonable set of dynamics for an "outer" altitude loop.

C. SURVEY OF K/s^2

The survey of K/s^2 (Table 7) indicates that this form of transfer function is less desirable than K/s. The control effectiven terms must be extremely high (K of the order of 4000) to achieve an error on the order of 1 ft^2. Moreover, the closed-loop natural frequency of approximately 65 rad/sec is somewhat high for an altitude outer loop.

TABLE 6. SURVEY OF K/s

K	$E(\delta^2)$	$E(h^2)$	Δ
10	15.96	20.1	s + 10
20	13.78	8.59	s + 20
30	9.6	3.25	s + 30
40	6.71	1.46	s + 40
100	1.5	0.074	s + 100

TABLE 7. SURVEY OF K/s^2

K	$E(\delta^2)$	$E(h^2)$	Δ
10	3.69	74.9	$(s + 2.24)^2 + (2.24)^2$
20	4.912	65.85	$(s + 3.2)^2 + (3.2)^2$
50	5.9	54.5	$(s + 5)^2 + (5)^2$
100	6.8	45.1	$(s + 7.1)^2 + (7.1)^2$
1000	6.2	6.13	$(s + 22)^2 + (22)^2$
4000	1.58	0.9	$(s + 45)^2 + (45)^2$

D. SURVEY OF K/s^3 AND K/s^4

For K/s^3, a value of $K = 10^5$ is required to produce $E(\delta^2) = 3.3$ and $E(h^2) = 5.8$ ft^2. The closed loop roots are

$$\Delta = (s + 46.4)[(s + 23.2)^2 + (40.2)^2] \tag{27}$$

For K/s^4, a value of $K = 10^8$ is required to produce $E(\delta^2) = 0.8$, $E(h^2) = 1.8$ ft^2 and

$$\Delta = [(s + 38.3)^2 + (92.4)^2][(s + 92.4)^2 + (38.3)^3] \tag{28}$$

E. IMPLICATIONS OF SYSTEM SURVEYS FOR AIRFRAME SELECTION

The K/s transfer function is indicated to be the most desirable form, since good performance is attained for a reasonably low value of K. We now examine the practical realizability of such a transfer function. As shown in Fig. 22 it is assumed that, in addition to the outer loop control δ_1, an additional control δ_2 is employed. In Fig. 22 δ_2 is denoted as "Flap", but δ_2 may in fact be a combination of several aerodynamic surface controls, e.g., for Configuration 6H a combination of front wing flaps and rear wing flaps. From Table 5 we put K=30 as a desirable value. Then, following the procedure of Ref. 1, p. 112, the crossfeed transfer function C_x is given by the solution of

$$\frac{30}{s} =$$

$$\frac{C_x Z_{\delta_2} s^2 - (M_q + M_{\dot{\alpha}})s - [M_\alpha - (M_{\delta_2}/Z_{\delta_2})Z_\alpha] + A_{h_{\delta_1}} s^2 + B_{h_{\delta_1}} s + C_{h_{\delta_1}}}{s^2(s^2 + Bs + C)} \tag{29}$$

where B, C, $A_{h_{\delta_1}}$, $B_{h_{\delta_1}}$, $C_{h_{\delta_1}}$ etc. are given in Table 1.

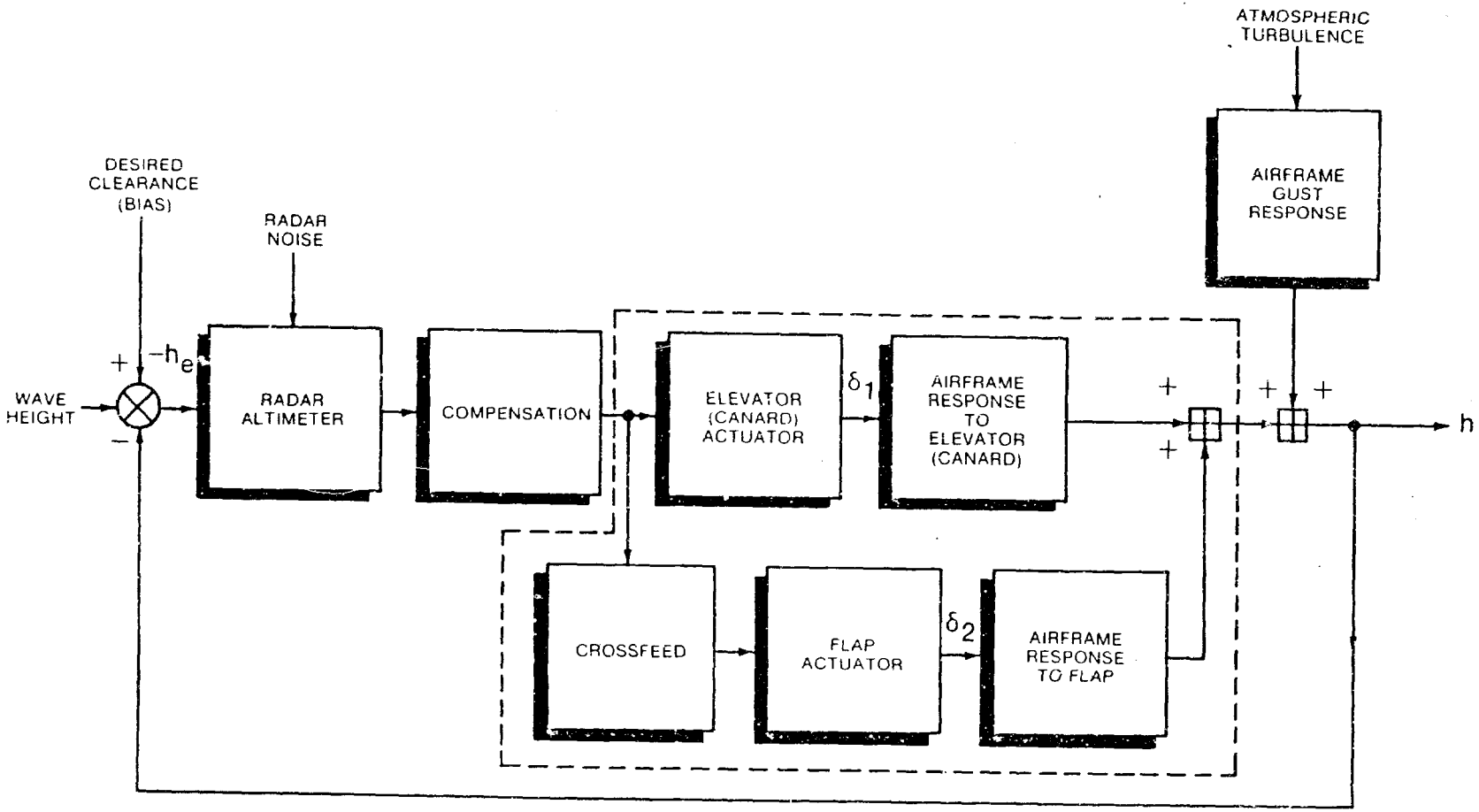

Figure 22. Multicontroller System Block Diagram

For Configuration 6H this yields

$$C = \frac{30s^3 + 30Bs^2 + 30C - A_{h_{\delta_1}}s^2 - B_{h_{\delta_1}}s - C_{h_{\delta_1}}}{Z_{\delta_2}\{s^2 - (M_q + M_{\dot{\alpha}})s - [M_\alpha - (M_{\delta_2}/Z_{\delta_2})Z_\alpha]\}} \tag{30}$$

$$C = \frac{30s^3 + 61.172s^2 + 179.3119s - 500.441103}{Z_{\delta_2}\{s^2 + 0.977s + 5.2488 - 864.77\ (M_{\delta_2}/Z_{\delta_2})\}} \tag{31}$$

For the crossfeed to be constructed physically C must not be unstable. This leads to the same condition on $M_{\delta_2}/Z_{\delta_2}$ as derived in Ref. 1, i.e.,

$$\frac{M_{\delta_2}}{Z_{\delta_2}} < \frac{5.248}{864.77}$$

or, approximately

$$\frac{M_{\delta_2}}{Z_{\delta_2}} < 0$$

which implies that the flap deflection which generates an increase in lift must also generate a nose-up pitching moment, or at least zero pitching moment. In other words, a "Direct Lift" type of control is necessary. This is more readily achieved with a joined wing or canard configuration than with a conventional aft tail configuration.

A second condition that must be met by the crossfeed transfer function is that C should be physically realizable. This implies that the numerator of C should be of equal or lower order than the denominator. Clearly, C, as calculated above does not meet this condition. It is therefore necessary to modify C by introducing additional high-frequency denominator terms. These additional terms will not seriously degrade the system performance, because the wave input peak frequency is relatively low (6.3 rad/sec).

SECTION VII

CONCLUSIONS

1. Optimal control theory of the Wiener-Hopf type can conveniently be applied to the design of cruise missile terrain-following guidance systems. For single-controller systems the optimal compensation transfer function is stable, but may have a numerator of higher order than its denominator. Thus, it must be approximated if it is to be physically constructed. The performance loss due to this approximation is small.

2. For multi-controller systems to achieve good performance at least one of the airframe control surfaces should provide either zero or nose-up pitching moment when the control is deflected so as to increase lift. This is more easily achieved by a joined wing or canard configuration than by a conventional aft tail configuration.

3. Of the three types of terrain considered (rolling terrain, rough terrain, and a short-crested sea) the short-crested sea provided the most severe operating environment, and required large control deflections for close terrain-following. The effect of atmospheric turbulence was relatively small.

4. Terrain-following systems designed by optimal control theory give appreciably better performance than those obtained by standard system design methods. When following the short-crested sea the latter systems give mean square errors greater than would have been obtained by flying at constant inertial altitude. The control system feedback laws for existing cruise missiles were not available to the authors, so it is not known how existing cruise missile guidance systems compare with the standard (non-optimal) systems analysed in this report. If existing cruise missile guidance systems employ any of the standard (non-optimal) feedback laws analysed in this report considerable improvements in terrain-following accuracy would be obtained by changing to optimal feedback laws.

REFERENCE

1. Wolkovitch, J., Application of the Joined Wing to Cruise Missiles, ONR-CR212-266-1, Nov. 1980.

2. Fortenbaugh, R. L., "Progress in Mathematical Modeling the Aircraft Operational Environment of DD 963 Class Ships," AIAA Paper 79-1677, 1977.

3. Cunningham, E. P., "Single-Parameter Terrain Classification for Terrain Following," J. Aircraft, Dec. 1980, p. 909-914.

4. Whitbeck, R. F., Wiener-Hopf Approaches to Regulator, Filter/Observer and Optimal Coupler Problems, Contract No. N00014-78-C-0391, ONR-CR215-260-1, Jan. 1980.

5. Whitbeck, R. F., "'Direct' Wiener-Hopf Solution of Filter/Observer and Optimal Coupler Problems," J. of Guidance and Control, Vol. 4, No. 3, May-June 1981, pp. 329-336.